QIRT10
http://dx.doi.org/10.21611/qirt.2010.034
10th International Conference on Quantitative InfraRed Thermography
July 27-30, 2010, Québec (Canada)

Shape and temperature field distortions induced by convective effect on hot object in the near infrared and infrared spectral bands

by A. Delmas* ** ***, Y. Le Maoult* **, JM. Buchlin***, T. Sentenac* **, and JJ. Orteu* **

** Université de Toulouse ; INSA, UPS, Mines Albi, ISAE ; ICA (Institut Clément Ader) ; F-81013 Albi Cedex 09, France (adelmas@enstimac.fr)*
*** Ecole des Mines d'Albi ; Campus Jarlard, F-81013 Albi, France*
**** The Von Karman Institute For Fluid Dynamics, Chaussée de Waterloo 72, 1640 Rhode Saint Genèse, Belgium*

Abstract

The goal of this paper is to point out the perturbation induced by convective effect (mirage effect) on shape and temperature measurement and to give an estimation of the error done. This work will explore the sensitivity of several spectral bands: 8-12μm, visible and recently the 0.75-1.7μm band (near IR) with the help of CCD camera (Si) or VisGaAs camera. Several methods will be used in order to highlight the phenomena and to obtain quantitative values of the error done. We will give the displacement and the deformation error for each spectral band.

1. Introduction

The ICA Mines Albi and VKI follows since numerous years works about IR radiometry with the aim to do quantitative thermography (true temperature measurement without contact). The ICA Mines Albi deals also on thermal-dimensional coupling measurements, and so needs to merge usual video data with infrared data. Studies done in this specific domain have underlined some perturbations emphasized at high-temperature (T>800°C) [1]. This work deals in details with treatment of some perturbations which play a role in the measurement of different parameters in the near IR band. We will focus in this study on perturbations which arises from convective effect present around high-temperature object [2,3]. Effectively, when a hot object is in a colder surrounding media, a temperature gradient is shaped around the object and so a refractive index gradient too (according to the Gladstone-Dale law). This phenomenon brings inevitably distortion of spatial informations received by the camera. The goal of this work will be in a first time to show clearly this effect and in a second time to estimate errors made on distortion and/or temperature measurement by CCD or VisGaAs camera on hot object. We illustrate the presence of distortion by experimental way (schlieren photography…) and numerical way (ray-tracing [4]). Then, we describe different methods used to estimate the convective effect on temperature and distortion measurement and we give our first results. Finally, some possible ways to correct pertubated images are given.

2. Mirage effect

The mirage effect appears as soon as we have a refractive index gradient. What we called mirage effect is when light beams do not arrive at the expected destination (without temperature gradient). Usually this effect does not have a big influence on optic measurement. But, if we are in presence of a strong refractive index gradient, the information measured can be wrong enough to be taken into account. In our case, the refractive gradient is engendered by a temperature gradient coming from a natural convective plume. Mirage effect induced by natural convection is very frequent and can be observed in numerous cases. The most famous one is the mirage effect which occurs over a road or in the desert when the sun is strongly hitting the ground.

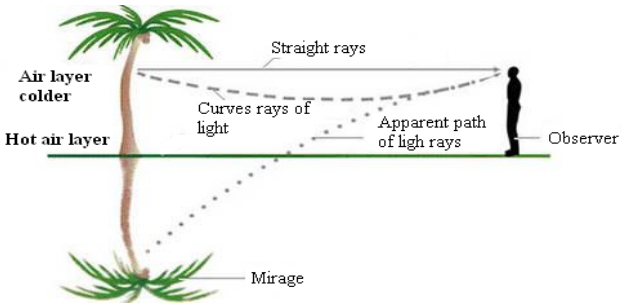

Fig. 1. *Mirage effect principle*

http://dx.doi.org/10.21611/qirt.2010.034
10th International Conference on Quantitative InfraRed Thermography

In our case, we will focus on mirage effect which occurs around hot object. It can be sometimes a real problem when we need to know with accuracy the shape or the temperature of a given point of the object. We give in this work a value of the error made when we are trying to make such measurement. In addition, the deflection induced by the temperature gradient varies with the wavelength. According to the Eq. (1) called Gladstone-Dale law [4], we can obtain for a given temperature field and wavelength, the index refraction distribution.

$$n_\lambda - 1 = K_\lambda . \rho(T) \quad (1)$$

$$\text{where } K_\lambda = \frac{N.\alpha_0}{2.\varepsilon_0} \text{ (m}^3\text{/kg)} \quad (2)$$

The Gladstone-Dale constant K is function of the wavelength λ (because α_0: polarizability of one molecule depends on λ), ε_0 is the vacuum permittivity and N is the Avogadro number. We choose to work first in the visible band, with the wavelength of the He-Ne laser: λ=652,8nm and K=0,2256.10^{-3} m^3/kg. In our case, air can be taken as an ideal gas, and so:

$$\rho = \frac{352{,}86}{T} \quad (3)$$

With combination of Eqs. (1) and (3), we establish for the specific wavelength of an He-Ne laser.

$$n - 1 = 0{,}079.T^{-1} \quad (4)$$

We can see in the figure 2 how the refractive index depends on the temperature and on the wavelength

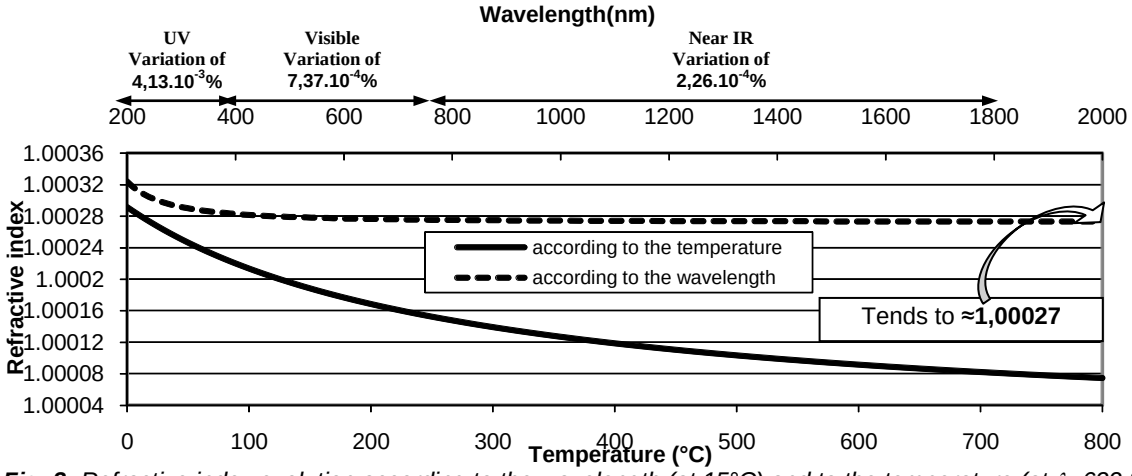

Fig. 2: *Refractive index evolution according to the wavelength (at 15°C) and to the temperature (at λ=632,8nm) [5]*

We are now able to obtain directly from the temperature field, the refractive index distribution for a given wavelength. The next step is then to deduct from this distribution, the displacement induced. A numerical approach based on a ray-tracing code has been used with the purpose to observe the phenomena and to obtain some value of displacement.

3. Numerical approach : Ray-tracing tools

This step of our work is divided in three parts. First, we compute the temperature field around the considerate object by means of the software FLUENT. Then, according to the Gladstone-Dale law, we deduce the refractive index field directly linked to the temperature for a given wavelength. Finally, we put this refractive field in our ray-tracing code, working on MATLAB. The study is made in a first step with simple geometry, as reference test case before to go on with more complex geometry. With this aim, we deal first with axisymmetric geometry (as cylinder or horizontal disk). Here, we show only result for the disk.

http://dx.doi.org/10.21611/qirt.2010.034

3.1. Fluent

To obtain the refractive index distribution necessary for the ray-tracing code, we need to know the temperature field around the studied object. We choose here to study the convective plume which appears above a horizontal heated disk of 9,2cm diameter. A cylindrical perturbation permits to create easily a good mirage effect, not only along x but also along y. We obtain with this device a laminar perturbation around 4,5cm width, 10cm above the disk. The temperature field is computed by numerical simulation with the software FLUENT. The simulation is made in axisymmetric; a rotation around the centre of the disk will give the entire temperature field. The figure 3 shows the 2D temperature map above a disk at 1000K (temperature of studied materials in the laboratory ICA range from ≈ 400K to 1700K, corresponding from polymers forming and thermal barriers processing and testing temperatures).

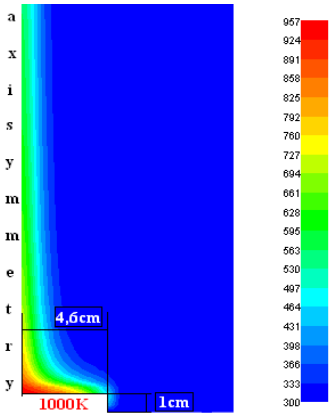

Fig. 3: *Temperature contours obtained with FLUENT*

3.2. Ray-tracing software

After to have converted the temperature field in refractive field thanks to the Eq. (4), we incorporate this data in our ray-tracing code [6] as the figure 4 illustrates it. The original plan is composed of radiating elements located with their y and z coordinates. Each element launches one ray perpendicularly to the original plan. The refractive index field is around and above the disk is discretized according to the radial and axial coordinates, *r* and *z* in order to create a large number of cells with constant refractive index. Transition from one cell to another is governed by the Snell-Descartes law (transition between a cell *i* to a cell *j* with n and θ respectively the refractive index of the cell and the angle between the ray and the normal to the surface of the cell surface):

$$n_i.\sin(\theta_i) = n_j.\sin(\theta_j) \qquad (5)$$

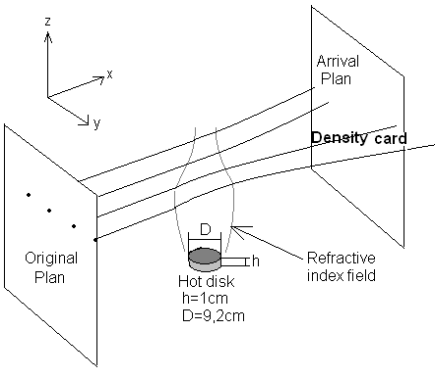

Fig. 4: *Diagram showing the functioning of the code and its geometry*

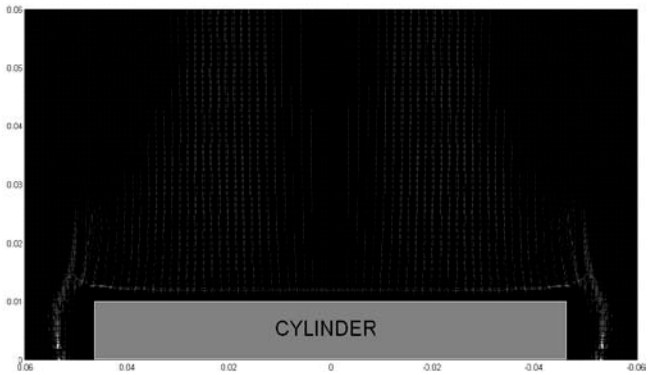

Fig. 5: *Density map after the passage of rays around and above the disk (1000K)*

Then, when the ray goes out of the last cell, so from the thermal perturbation, it continues his path until the arrival plan, which the position according to x can be adjusted to accentuate the distortion effect. Indeed, the further the screen is, the more the deviation is.

http://dx.doi.org/10.21611/qirt.2010.034
10th International Conference on Quantitative InfraRed Thermography

If we discretize sufficiently the original plan and enough rays are launched, here 340000 to obtain the figure 5), we obtain on the arrival plan a density map which show convergence zones of rays or at the opposite, dark zones, corresponding to regions where few or none rays arrive. The figure 5 provides an example of result get for the case of the disk heated at 1000K, with the arrival plan located at 5m behind the center of the disk and for the specific wavelength of the He-Ne laser (λ=652,8nm). It shows the distortion effect, every ray passing near the edge of the disk goes towards colder temperature (higher refractive index) creating the dark zone. Consequently, we obtain a convergence zone (more clear) corresponding to rays missing in the dark zone. Above the disk we can also notice that rays passing close to the center are not deviated, which is in agreement with Snell-Descartes law.

4. Comparison of the convective plume geometry between numerical approach and schlieren photography

Schlieren photography is a visual process that is used to photograph the fluids flow of varying density. The basic optical schlieren system uses light from a single collimated source shining on a target object. Variations in refractive index causes by density gradients in the fluid distort the collimated light beam. This distortion creates a spatial variation in the intensity of the light, which can be visualised directly with a shadowgraph system (figure 6).

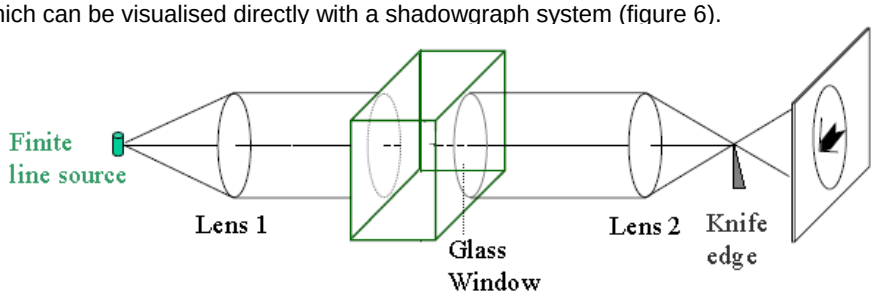

Fig. 6: *Diagram of the Schlieren photography technique*

In schlieren photography, the collimated light is focused with a lens, and a knife-edge is placed at the focal point, positioned to block about half the light. In flow of uniform density this will simply make the photograph half as bright. However in flow with density variations the distorted beam focuses imperfectly and parts which have been focused in an area covered by the knife-edge are blocked. The result is a set of lighter and darker patches corresponding to positive and negative fluid density gradients in the direction normal to the knife-edge. The sensitivity of the schlieren device is adjusted moving the knife-edge more or less in the focal point. In the case of our heated disk, we obtain the following pictures:

Fig. 7: *Schlieren photography pictures for several surface temperature*

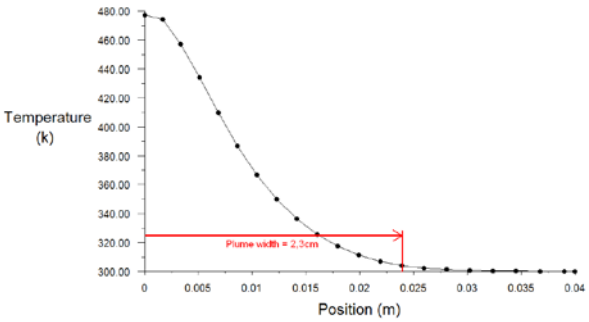

Fig. 8: *Plume width measured with FLUENT at 10 cm*

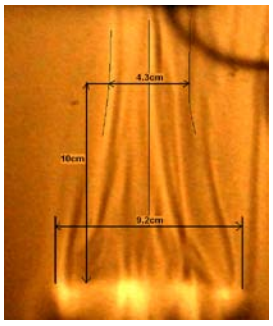

Fig. 9: *Plume width measured with schlieren photography*

http://dx.doi.org/10.21611/qirt.2010.034

As we can see in the figure 7, the perturbation above the disk is more or less the same. We notice first the development of the boundary layer from the edge of the disk toward the center. Then, near the center the flow must separate to form a plume. If undisturbed, the plume will be a steady flow whose energy transport rate is equal to the heat transfer rate from the disk surface. Theoretically, the plume width (at a given elevation) should decrease with increased source strength [7]. But the main problem which occurs here is the heating of the disk support with time. That's why the picture is more pertubated for high temperature. Moreover, natural convection coming from under the disk can be seen, going up straight from the edge of the disk. A comparison with results obtain with FLUENT has been made in order to validate its. We have compared, for a given temperature surface (650K), the plume width at a given elevation (see figure 8 and 9). The width measured with FLUENT and with the schlieren photography are respectively of 4,6cm and 4,3cm. The difference between the two techniques is about 6%. We can assume that the result obtain with FLUENT correspond to the real case and so that we put real field of refractive index in the ray-tracing code. We notice finally that, whatever the disk temperature, the flow stay laminar ($Gr<10^8$). Obstacles should be added in order to agitate the plume, and simulate a turbulent flow.

5. Experimental approach

5.1. Displacement measurement method

5.1.1. Principle of the Background Oriented Schlieren method

Background Oriented Schlieren (BOS) [8] is a novel technique for flow visualization of density gradients in fluids using the Gladstone-Dale relation between density and refractive index of the fluid. BOS simplifies the visualization process by eliminating the need for the use of expensive mirrors, lasers and knife-edges. In its simplest form, BOS makes use of simple background patterns of the form of a randomly generated dot-pattern. In its initial stages of implementation, it is mostly being used as a qualitative visualization method. But in our case, thanks to a PIV software, we are able to obtain a quantitative displacement. The figure 10 gives the working of the BOS method:

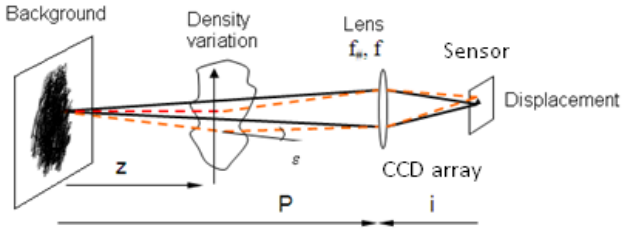

Fig. 10: *Diagram explaining the BOS technique*

The density variation comes from the disk and is created in a plexiglas enclosure (40cm*30cm in surface and 1m high) in order to avoid external perturbations (see picture in figure 13). The disk is heated by a wire resistance bamboozled under a steel disk and needs a supply of 13A and 40V. To obtain result of displacement, two images of the background are recorded, one with perturbation and one without. Then, an analysis of these images is made in order to deduct the displacement of each element from the dot-pattern. This analyze is realized with the help of the software WIDIM (Window Displacement Iterative Multigrid) [9], software developed by the Von Karman Institute and usually utilized in PIV. WIDIM makes a cross-correlation between the two pictures and gives as result the displacement of each element in pixel along the *x* direction and *y* direction.

5.1.2. Results

Results can be represented as a displacement map of each element of the background in order to see where the displacement occurs. The picture of the background has been taken passing through the perturbation right above the disk.

5.1.2.1. Visible spectral band

In this case the distance Z is 1m and P 1,6m. The lens used has a focal distance of 50mm. The camera is a Pixelfly QE model with a CCD sensor resolution of 1392x1036.

As we can see in the figure 11, we obtain a displacement maximum around 10 pixels close to the disk and around 5 pixels in the plume, which are respectively a displacement of 2,4mm and 1,2mm on the board. We can notice that in the center of the plume (the center of the plume is also in the center of the sensor so around the pixel number 680) we do not have a displacement. It's in agreement with what we have seen with the numerical approach of ray-tracing.

http://dx.doi.org/10.21611/qirt.2010.034
10th International Conference on Quantitative InfraRed Thermography

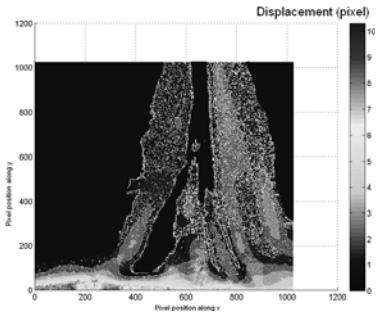

Fig. 11: *Displacement map above the disk in the visible band*

5.1.2.2. Near Infrared spectral band (preliminary results)

In this case the distance Z is 1m and P 1,25m. The lens used has a focal distance of 75mm. And the resolution of the sensor is 320x256. The camera used is a Xenics camera with VisGaAs CCD sensor working from 0,75μm to 1,7μm. The light used to illuminate the pattern comes from an incandescent lamp with filter window centered around 830nm. As for the experiment shown in 5.1.2.1., we obtain the maximum displacement right above the disk with a displacement of 7 pixels, or 3,5mm on the pattern. However, to be able to measure a displacement big enough (because of the poor resolution of IR camera) we had no choice to use a lens with bigger focal distance.

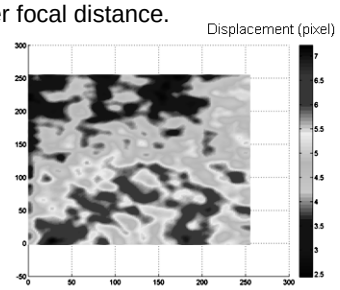

Fig. 12: *Displacement map above the disk in the near infrared band*

5.1.2.3. Far Infrared spectral band (preliminary results)

For the infrared camera the BOS method is revealed impossible to apply. The resolution of the camera is too big to allowing the detection of small random point. The numerical resolution is 280x280 and the angle of view is 20°. The distance Z is 25cm and P 50cm. The camera is an AGEMA 880 LW with scanning device and cold by stirling cycle. We use in this case big black circle on a white paper. We warm the paper with incandescent lamp. Black circles absorb more than white circle and become hotter, the difference of temperature permits to detect enough circles edge. Then, with a code written in MATLAB we can determine the center of the circle and so obtain the displacement between two pictures. The displacement measured is around 0,4 pixel, or on the pattern 0,18mm.

5.2. Distortion measurement method

5.2.1. Principle of the distortion measurement method

The distortion field measurement is often used when we want to control the material forming, that is to say when we want to confer to a piece (generally metallic) a specific shape in a given range of tolerance. It needs so to find a distortion measurement system which allows to compare the success of the forming. For this purpose, it's common to use forms predefined, drawn on the piece before the constraint application. We chose in our study to use circles, which will become ellipses during the distortion [10]. As the BOS method, the technique is to observe the background with and without perturbation and then to analyze the recorded picture. Once that we have the two recorded pictures, we realize an image processing in order to obtain ellipses parameters needed to compute the distortion. Distortions along *x* and *y* (ε_x and ε_y) are respectively calculated by these following equations:

$$\varepsilon_x = \ln\left(\frac{a}{r}\right) \text{ and } \varepsilon_y = \ln\left(\frac{b}{r}\right) \quad (6)$$

http://dx.doi.org/10.21611/qirt.2010.034

With *r* the initial radius of the circle and *a* and *b* the radius of the ellipse respectively along *x* and *y*.

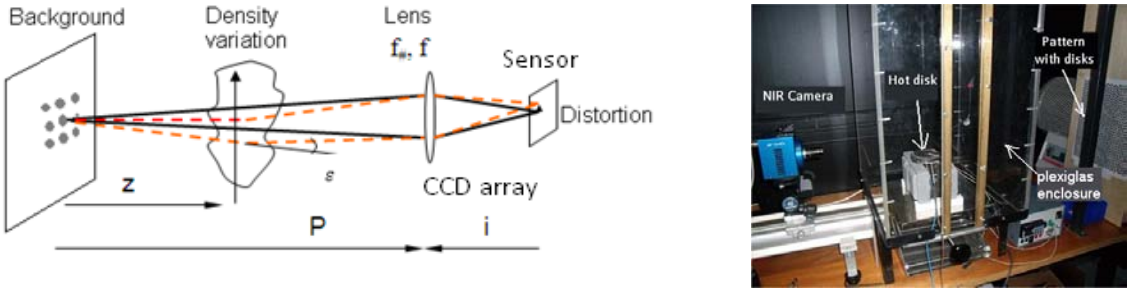

Fig. 13: Diagram and photo explaining the distortion measurement method

5.2.2. Results

Results can be represented as a distortion map of each element of the background in order to see where the distortion occurs. The picture of the background has been taken passing through the perturbation right above the disk.

5.2.2.1. Visible spectral band

Like for the displacement measurement, the distance z is 1m and P 1,25m. The lens used has a focal distance of 50mm. And the resolution of the sensor is 1392x1036.

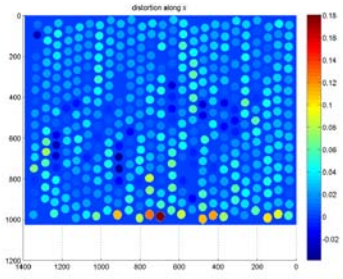

Fig. 14: *Distortion along x*

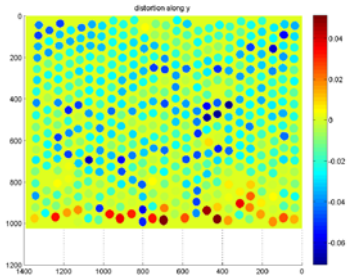

Fig. 15: *Distortion along y*

The distortion along x goes from -0,02 (far from the disk) to 0.18 (close to the disk). The distortion along x is more positive than negative because the perturbation inducts ellipse with longer radius along x than the initial circle. Along y, the distortion goes from -0,07 (far from the disk) to 0,05 (close to the disk). We can see in both cases that ellipses close to the disk have distortion more positive than negative. We can deduct of this result that the high temperature right above the disk produce a magnifier effect of ellipses.

5.2.2.2. Near Infrared spectral band (preliminary results)

Like for the displacement measurement, the distance z is 1m and P 1,25m. The lens used has a focal distance of 75mm. And the resolution of the sensor is 320x256.

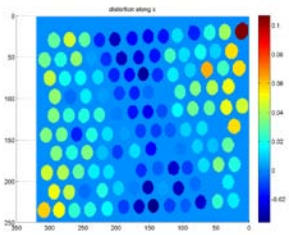

Fig. 16: *Distortion along x*

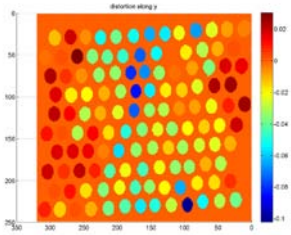

Fig. 17: *Distortion along y*

Figure 16 and 17 show that the distortion along *x* is not very important in the center of the plume whereas it is along *y*. It can be explained by the fact that the temperature field shape is made in the way that rays are not deflected along *x* in the center but along *y* (see Eq. 5)

5.2.2.3. Far Infrared spectral band (preliminary results)

In the far infrared band, the dark disk edges were not sharp enough to give acceptable result. So, we don't have yet suitable values to show in this part.

5.3. Error on the temperature (preliminary results)

In this part, we give an estimation of the error made when we want to make a temperature measurement through a perturbation of hot air. To do this, we simply observe a stabilized black body. We write down the value and then we put the perturbation between the black body and the camera. We observe in both cases (near infrared and far infrared) an increase of the temperature measured. The temperature of the black body in near infrared was 473K and 323K in far infrared. The error estimated is about the same in near and far infrared and is around 0,9K (big enough to be detected). This result is a preliminary result and more experiments have to be made to validate this value.

6. Conclusion and perspectives

The study done here has pointed out the mirage effect phenomena in several spectral bands and has started to give some quantitative information about the displacement and the distortion induced by the perturbation. We showed that the displacement is about 3mm for the visible and near infrared bands, and much more little for the far infrared band with around 0,2mm. These results are in agreement with the chart shown in the figure 2. The distortion measurement shows that the mirage effect can induce more than a displacement and can enlarge or narrow a motif. However, improves has to be made on our experiment to allow a good measurement in all the spectral bands (particularly in the infrared band). One of the further works will be to work on a periodic pattern in order to have an accurate displacement with a possibility to study amplitude and phase [11]. Moreover, the error made in temperature measurement has to be validated and we have to know precisely the role of CO2/H20 absorption and reflection in each spectral band. A numerical simulation of this experiment with our ray-tracing code will be also completed to see the part of the black body radiation arriving to the sensor. Then, the finally step is to correct pertubated images and to obtain images without perturbation coming from refractive index gradient. In the case of a laminar convection, the ray-tracing code can be used to predict the deviation of each point. But for a turbulent flow, a statistic analysis will be realized in an attempt to correct images.

REFERENCES

[1] Claudinon S., "Contribution à l'étude des distorsions au traitement thermique",Thèse Ecole des Mines de Paris, 2000.
[2] Badoz J., Fournier D., Boccara A. C., "Photoacoustics : a hundred years old technique revisited", Journal Optics 11, pp 399-408, 1980.
[3] El Motassadeq A., Chechouani H., Waqif M., Benet S., "Simulation des effets de la refraction dans la couche limite thermique au-desus d'un disque horizontal", Congrès français de thermique, 2000.
[4] Mayinger F., Feldmann O., "Optical measurements 2nd edition", Springer, 2001.
[5] Lide D. R., "Handbook of Chemistry and Physics 88th", 10-253, 2007-2008.
[6] Cosson B., Schmidt F., Le Maoult Y., Bordival M., "Infrared heating stage simulation of semi-transparent media (PET) using ray-tracing method", submitted to International Journal of Material Forming, November 2009.
[7] Robinson S.B., Liburdy J;A., "Prediction of the Natural Convective heat transfer from a horizontal heated disk", Journal of Heat transfer, Vol. 109, November 1987.
[8] Klinge F., "Investigation of background oriented schlieren towards a quantitative density measurement system", project report 19, Von Karman Institute, 2001.
[9] Scarano F., Riethmuller M. L., "Iterative Multigrid approach in PIV image processing with discrete window offset", Experiment in Fluids 26, pp 513-523, 1999.
[10] Morestin F., Bogaert P., Boivin M., "Mesure de deformation par imagerie", Colloque Photomécanique 95, ENS Cachan (France), pp 195-202, Ed. Eyrolles, 1995.
[11] Surrel Y., "La technique de la grille pour la mesure de champs de déplacements et ses applications", Photomécanique 4, p 193-216, 2004.